J. Plasma Fusion Res. SERIES, Vol. 6 (2004) 35–39

Relaxation Oscillations and Transport Barrier Dynamics in Tokamak Edge Plasmas

BENKADDA Sadruddin, BEYER Peter, FUHR-CHAUDIER Guillaume,
GARBET Xavier[1], GHENDRIH Philippe[1] and SARAZIN Yanick[1]
Equipe Dynamique des Systèmes Complexes, Laboratoire PIIM
CNRS – Université de Provence, Marseille, France
[1]Association Euratom – CEA, CEA/DSM/DRFC CEA Cadarache, France
(Received: 9 December 2003 / Accepted: 25 February 2004)

Abstract

Oscillations of turbulent transport of particles and energy in magnetically confined plasmas can be easily observed in simulations of a variety of turbulence models. These oscillations typically involve a mechanism of energy exchange between fluctuations and a poloidal shear flow. This kind of "predator-prey" mechanism is found to be not relevant for transport barrier relaxations. In RBM simulations of resistive ballooning turbulence with transport barrier, relaxation oscillations of the latter are observed even in the case of frozen poloidal shear flow. These relaxations are due to a transitory growth of a mode localized at the barrier center. A one-dimensional model for the evolution of such a mode in the presence of a shear flow describes a transitory growth of an initial perturbation. Oscillations in the case of a finite steady-state shear flow are possible due to the coupling of the mode to the dynamics of the pressure profile.

Keywords:

relaxation oscillation, transport barrier, ELMs, plasma turbulence

1. Introduction

Relaxation oscillations in fusion plasmas have a strong impact on energy and particle confinement. The most promising operational regime of future reactors is characterized by the existence of a transport barrier at the plasma edge. This barrier is not stable but relaxes quasi-periodically. During such fast relaxation events, turbulent transport through the barrier increases strongly and the pressure inside the barrier drops. Thereafter, the barrier builds up again on a slow, collisional time scale. These relaxation oscillations are linked to so called edge localized modes (ELMs) which are believed to be magneto-hydrodynamical (MHD) modes driven by the edge pressure gradient (ballooning) and/or the edge current (peeling) [1].

The basic physical mechanism underlying these kind of relaxation oscillations is not yet understood. In particular, there is no explanation why the plasma, in stead of remaining in a statistically stationary state close to pressure gradient or edge current stability limits, crosses these limits quasi periodically.

A possible mechanism for oscillations of turbulent flux in confined plasmas is based on the dynamics of poloidal flows that are generated self-consistently by turbulent fluctuations. These flows stabilize the turbulence. Therefore, oscillations are in principle possible due to a periodic exchange of energy between the fluctuations and the poloidal flow [2,3,4]. In this first part of this article, we will show that such oscillations can be observed in simulations of resistive ballooning mode (RBM) turbulence at the collisional edge of a tokamak plasma. Furthermore, it is possible to construct one-dimensional or zero-dimensional models for this kind of dynamics.

However, as we will show in the second part of this article, relaxation oscillations of transport barriers can be observed even with frozen poloidal flow. In this case, a steady state shear flow is imposed externally to generate the barrier, but the flow does not participate in the dynamics. The relaxations are due to a transitory growth of a mode localized at the center of the barrier. Such a transitory growth is found to be consistent with shear flow stabilization.

2. Model for resistive ballooning turbulence

Resistive ballooning mode (RBM) turbulence at the collisional edge of a tokamak plasma is modeled by reduced resistive MHD equations for the normalized electrostatic potential ϕ and pressure p [5,6],

$$\partial_t \nabla_\perp^2 \phi + \left\{ \phi, \nabla_\perp^2 \phi \right\} = -\nabla_\parallel^2 \phi - \boldsymbol{G} p + \nu \nabla_\perp^4 \phi \,, \qquad (1)$$

Corresponding author's e-mail: benkadda@up.univ-mrs.fr

$$\partial_t p + \{\phi, p\} = \delta_c \boldsymbol{G}\phi + \chi_{\|}\nabla_{\|}^2 p + \chi_{\perp}\nabla_{\perp}^2 p + S\,. \qquad (2)$$

Equation (1) corresponds to the charge balance in the drift approximation involving the divergences of the polarization current, the parallel current, and the diamagnetic current, and effects due to a viscosity ν, respectively. Equation (2) represents the energy balance, where $\chi_{\|}$ and $\chi_{\perp}$ are effective parallel and perpendicular collisional heat diffusivities and $S(r)$ is an energy source. The curvature operator $\boldsymbol{G}$ arises from the compressibility of diamagnetic current and $\boldsymbol{E}\times\boldsymbol{B}$ drift. In this MHD model, the diamagnetic velocity is neglected with respect to the $\boldsymbol{E}\times\boldsymbol{B}$ velocity, and the parallel current is evaluated using a simplified electrostatic Ohm's law, $\eta_{\|0} j_{\|} = -\nabla_{\|}\phi$ (in dimensional units), where $\eta_{\|0}$ is a reference value of the parallel resistivity.

The system (1, 2) has been normalized using the resistive interchange time τ_{int} and the resistive ballooning length ξ_{bal} with $\tau_{int}^2 = R_0 L_p/(2c_{S0}^2)$ and $\xi_{bal}^2 = m_i n_0 \eta_{\|0} L_s^2/(\tau_{int} B_0^2)$. Here, R_0, L_p, and L_s are characteristic values of the major radius, the pressure gradient length, and the magnetic shear length, respectively, $c_{S0} = [p_0/(m_i n_0)]^{1/2}$ is the sound speed calculated with reference values of the pressure p_0 and the density n_0, m_i is the ion mass, and $\delta_c = (5/3)2L_p/R_0$. Time is normalized to τ_{int} and the perpendicular and parallel length scales are given by ξ_{bal} and L_s, respectively. Electrostatic potential and pressure are normalized to $B_0\xi_{bal}^2/\tau_{int}$ and $\xi_{bal} p_0/L_p$, respectively.

The geometry of magnetic flux surfaces corresponds to a set of circular concentric tori, (r, θ, φ) being the labels of minor radius, poloidal and toroidal angles. The Poisson bracket is $\{\phi, \cdot\} = r^{-1}(\partial_r\phi\partial_\theta - \partial_\theta\phi\partial_r)$, the curvature operator is $\boldsymbol{G} = \sin\theta\partial_r + \cos\theta r^{-1}\partial_\theta$ and the gradient along field lines is $\nabla_{\|} = \partial_\varphi + q^{-1}\partial_\theta$. RBM turbulence is expected to be relevant in collisional edge plasmas. Assuming a monotonically increasing safety factor $q(r)$, the domain chosen for the study of RBM turbulence typically covers a region between $q = 2$ and $q = 3$ at the plasma edge.

3. Oscillations with poloidal flow dynamics

In full three-dimensional numerical simulations of the system (1, 2), oscillating states can be found where kinetic energy is periodically exchanged between fluctuating components $\vec{\tilde{u}}$ of the $\boldsymbol{E}\times\boldsymbol{B}$ velocity and the poloidal flow $\bar{u}$. The latter are defined by

$$\bar{u}_\theta \hat{e}_\theta = \langle \vec{u} \rangle\,, \quad \vec{\tilde{u}} = \vec{u} - \bar{u}_\theta \hat{e}_\theta\,, \quad \text{with} \qquad \vec{u} = \vec{u}_{E\times B}$$

and

$$\langle \cdot \rangle = \frac{1}{4\pi^2}\int_0^{2\pi}\int_0^{2\pi} \mathrm{d}\theta\,\mathrm{d}\varphi\,,$$

where $\hat{e}_\theta$ is the unit vector in the poloidal direction. A typical example is shown in Fig. 1. By performing a proper orthogonal decomposition [7,8] of the spatio-temporal fields of velocity and pressure, it is possible to determine the spatial structures relevant for the dynamics. A subsequent Galerkin projection then provides a system of ordinary differential equations for the amplitudes of these structures. Such a reduced model is given by [2],

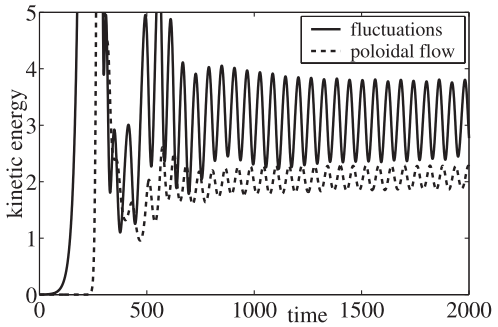

Fig. 1 Time evolution of the kinetic energy of fluctuations and poloidal flow in a 3D simulation of RBM turbulence, initialized with an unstable pressure profile and small fluctuations.

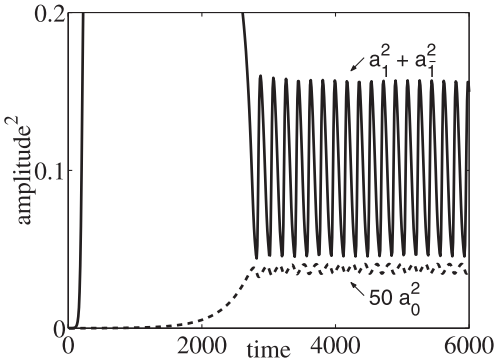

Fig. 2 Time evolution of two fluctuating modes (a_1, $a_{\bar{1}}$) and the poloidal flow a_0 in an oscillating state.

$$\begin{aligned}
\dot{a}_0 &= -\epsilon\gamma_0 a_0 + \epsilon\gamma_0 a_1 a_{\bar{1}} \\
\dot{a}_1 &= \gamma_1 a_1 - a_0 a_{\bar{1}} - \nu_1 a_{\bar{1}}^2 a_1 - \nu_2 a_1^3 \\
\dot{a}_{\bar{1}} &= -\gamma_{\bar{1}} a_{\bar{1}} + a_0 a_1 - \nu_1 a_1^2 a_{\bar{1}}
\end{aligned} \qquad (3)$$

Here, a_1 and $a_{\bar{1}}$ are the amplitudes of the most important spatial structures of the fluctuations $\vec{\tilde{u}}$, and a_0 is the amplitude of the relevant radial profile of the poloidal flow $\bar{u}$. γ_1, $\gamma_{\bar{1}}$, $\epsilon\gamma_0 > 0$ are linear growth rates, ν_1, ν_2 are coefficients, and ϵ is a small parameter. As can be seen in Fig. 2, the system (3) reproduces qualitatively the oscillations observed in the full system (1, 2). Note that if one freezes the dynamics of the amplitude a_0, i.e. $\dot{a}_0 = 0$, the system always converges to a stable fixed point. In other words, the dynamics of a_0 is crucial for the oscillating solution of (3) even if the oscillations of the amplitude a_0 itself are not very pronounced.

4. Dynamics of transport barriers

In the RBM turbulence model, a transport barrier can be generated by externally imposing a locally sheared $\boldsymbol{E}\times\boldsymbol{B}$ flow. This flow locally reduces turbulent transport [9,10,11, 12,13,14]. As a consequence of the total energy flux conservation, the pressure gradient steepens in the shear layer. This mechanism is similar to the one observed experimentally when generating a transport barrier by edge biasing

[15,16,17]. The external drive of the shear flow is included by modifying the equation for the poloidal flow profile, $\bar{u}$, that follows from the magnetic flux surface average of eq. (1),

$$\partial_t \bar{u}_\theta = -\frac{1}{r^2}\partial_r r^2 \left\langle \tilde{u}_\theta \tilde{u}_r \right\rangle + \nu \partial_r \frac{1}{r}\partial_r r \bar{u}_\theta - \mu\,(\bar{u}_\theta - U)\,, \quad (4)$$

where the first terms on the right hand side correspond to the divergences of the Reynolds stress and the viscosity stress, respectively, and the last term has been added artificially to account for the friction with an external flux U. The latter is chosen to be strongly sheared at the reference position $r_0 = r_{q=2.5}$. In case of a large friction coefficient $\mu \to \infty$, the poloidal flow $\bar{u}_\theta$ tends to the external flow U. For finite μ, the Reynolds stress drive of the poloidal flow [18,19,20] is important.

In typical simulations of RBM turbulence with a transport barrier, the latter is not steady state but relaxes intermittently. This can be seen from Fig. 3a where time evolutions of the edge energy confinement time $\tau_{Eedge}(t)$, the turbulent flux at the barrier center $\langle u_r p\rangle(r_0, t)$ and the poloidal flow shear at the barrier position $\partial_r \bar{u}_\theta(r_0, t)$ are presented in a typical simulation. The edge confinement time is defined as the ratio of the energy confined in the volume considered and the total energy flux across a magnetic surface. It represents a measure for the "strength" of the barrier. As can be seen from Fig. 3a, the evolution of the confinement time is characterized by phases of a slow increase quasi periodically interrupted by rapid crashes. The latter correspond to relaxations of the barrier and are associated to large peaks of the turbulent flux at the barrier center as well as fluctuations of the velocity shear at the barrier position.

These relaxation oscillations persist even if the poloidal flow profile is frozen. Fig. 3b shows the corresponding results from a simulation with the same parameters as in Fig. 3a except that the friction coefficient is set to $\mu \to \infty$. In practice, this is achieved by suppressing artificially the Reynolds stress term in eq. (4). In this case, the velocity shear profile is constant in time but intermittent flux peaks with relaxation of the barrier do appear.

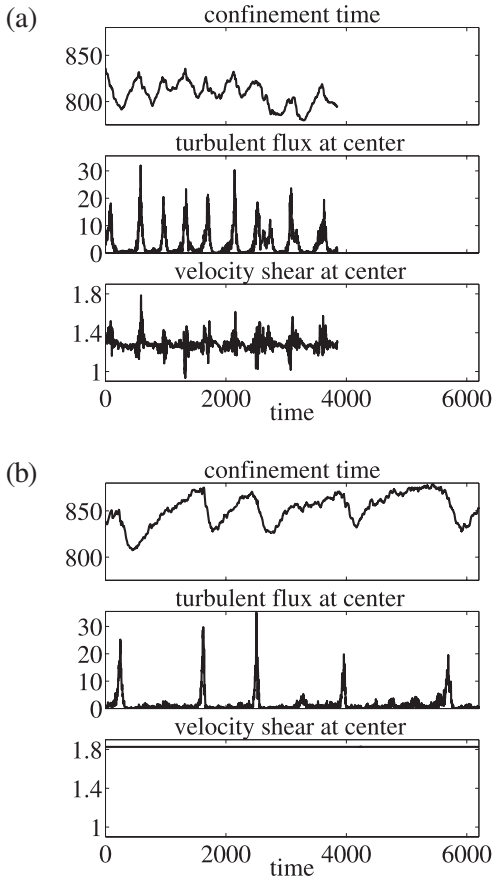

Fig. 3 Time evolution of confinement time, turbulent flux at the barrier center and poloidal velocity shear at the barrier center. In case (a), the poloidal flow fluctuates around the imposed flow due to the Reynolds stress. In case (b), the latter is suppressed artificially and the poloidal flow is frozen.

5. Possible mechanisms for barrier relaxations

As the relaxation oscillations shown in Fig. 3b appear in the case of a frozen poloidal shear flow, the mechanism of energy exchange between fluctuations and the poloidal flow is not relevant for these relaxation oscillations. Other possible mechanisms can either be excluded or seem to be not relevant:

- As the resistive ballooning instability is a threshold instability, it could be possible that the growth of a central Fourier component is triggered when the local pressure gradient at the barrier position passes a threshold. However, looking at the time evolution of this local pressure gradient, it often saturates before the barrier crash, and no clear sign of passing a threshold before the event can be observed.
- The strong velocity shear at the barrier center can in principle generate a Kelvin-Helmholtz instability. In contrast to the resistive ballooning instability, this type of instability is independent of the magnetic curvature. However, if the magnetic curvature is put to zero during our simulation, all turbulent fluctuations rapidly die out.

6. Shear flow stabilization

Linearizing the pressure equation (2) for a perturbation $p_{mn}(r, t)\,e^{im\theta - in\varphi}$, supposing a mean poloidal flow with constant shear, $\bar{u}_\theta = \omega_E(r - r_0)$ and replacing the coupling to the potential equation (1) by an instability term characterized by a growth rate γ_0, one obtains the linear evolution equation,

$$\partial_t p_{mn} + ik_\theta \omega_E x p_{mn} = \gamma_0 p_{mn} - \omega_t x^2 p_{mn} + \chi_\perp \partial_x^2 p_{mn}\,, \quad (5)$$

with $x = r - r_0$, $k_\theta = m/r_0$, and $\omega_t = \chi_\parallel/(r_0 L_s)^2$, where L_s is the shear length. The parallel gradient has been evaluated for a Fourier mode localized at the barrier center $\nabla_\parallel p_{mn} = ix/(r_0 L_s)\, p_{mn}$. In the absence of magnetic shear, one can calculate analytically the time evolution according to eq. (5) of an initial perturbation infinitely localized in space and time. A solution of the equation

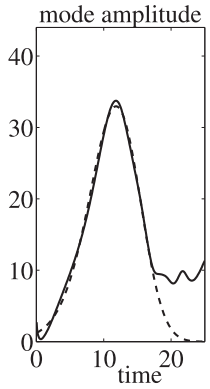

Fig. 4 Time evolution of the mode (m, n) = (5, 2) at the center of the barrier in a full 3D simulation started with a perturbation of this mode (full line) and analytical solution calculated from (7) (dashed line).

$$\partial_t p_{mn} + \mathrm{i}k_\theta \omega_E x p_{mn} = \gamma_0 p_{mn} + \chi_\perp \partial_x^2 p_{mn} + \hat{S}\delta(x)\delta(t)\ , \quad (6)$$

is given by

$$p_{mn} = \frac{\hat{S}}{\sqrt{4\pi\chi_\perp t}} \exp\left(-\frac{x^2}{4\chi_\perp t} + \frac{\mathrm{i}k_\theta \omega_E x}{2} t \right) \times \exp\left(\gamma_0 t - \frac{t^3}{3\tau_D^3} \right), \quad (7)$$

where $\tau_D = [\frac{1}{4}\chi_\perp (k_\theta \omega_E)^2]^{-1/3}$. Note that for $\omega_E = \gamma_0 = 0$, the usual solution of the diffusion equation is recovered. The solution (7) describes an initial transient growth of the perturbation for $t < \tau_D$ before the cubic term in the last exponential takes over the linear term, leading to a stabilization. The characteristic time for the transient growth is large for small values of the perpendicular diffusivity $\chi_\perp$ (close to the collisional value at the barrier center) and low poloidal wave numbers k_θ.

For a typical simulation such as the one shown in Fig. 3, we have $\tau_D \sim 10$ in normalized units for the central (m, n) = (5, 2) mode. A transient growth of this mode is found when starting a simulation with the corresponding pressure and velocity profiles, a perturbation of the (m, n) = (5, 2) component and small noise on all other components (Fig. 4). The peak of the mode amplitude is well reproduced by the expression (7). The dashed curve in Fig. 4 shows the graph of $p_{mn} = \hat{p}\ \exp[\gamma_0 t - t^3/(3\tau_D^3)]$, with $\hat{p} = 1.2$, $\gamma_0 = 0.42$, and $\tau_D = 10$.

7. 1D model for oscillations with frozen shear flow

Considering one dominant (m, n) mode, a reduced system for the radial dynamics of this mode coupled to the dynamics of the profiles can be obtained using the representation

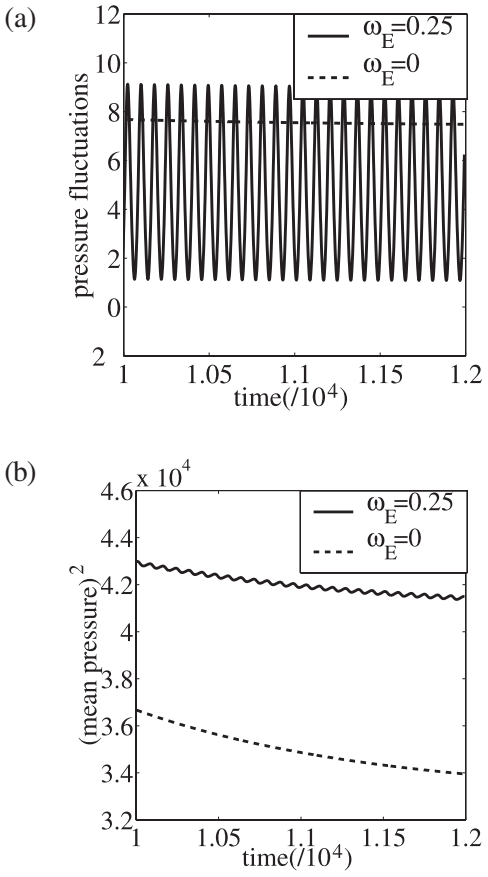

Fig.5 Time evolution of the rms pressure fluctuations $(\int \tilde{p}^2 \mathrm{d}r)^{1/2}$ (a) and the (squared) mean pressure $\int \bar{p}^2 \mathrm{d}r$ (b) according to eqs. (9, 10) with and without imposed shear flow.

$$\begin{pmatrix} \phi \\ p \end{pmatrix} = \begin{pmatrix} \bar{\phi} \\ \bar{p} \end{pmatrix}(r,t) + \begin{pmatrix} \tilde{\phi} \\ \tilde{p} \end{pmatrix}(r,t) \exp(\mathrm{i}m\theta - \mathrm{i}n\varphi) \quad (8)$$

and a subsequent Galerkin projection of the evolution equations (1, 2). The resulting system for the fields $\bar{\phi}$, $\tilde{\phi}$, $\bar{p}$, $\tilde{p}$ is simplified further by assuming a fixed relation between $\tilde{\phi}$ and $\tilde{p}$ given by the linear mode structure: $\tilde{\phi} = \mathrm{i}(\gamma_0/k_\theta)\tilde{p}$. Imposing a poloidal shear flow of the form $\partial_r \bar{\phi} = \bar{u}_\theta = \omega_E x$, a 1D model is obtained that consists of the equation (5) for the amplitude of the perturbation $\tilde{p}$ coupled to the dynamics of the pressure profile $\bar{p}$,

$$\partial_t \tilde{p} = -\mathrm{i}k_\theta \omega_E x \tilde{p} + \gamma_0(\partial_t \bar{p})\tilde{p} - \omega_t x^2 \tilde{p} + \chi_\perp \partial_x^2 \tilde{p} \quad (9)$$

$$\partial_t \bar{p} = -\gamma_0 \partial_x |\tilde{p}|^2 + \chi_\perp \partial_x^2 \bar{p} + S \quad (10)$$

In absence of a shear flow ($\omega_E = 0$), the system (9, 10) evolves to a stationary state. However, in the presence of a static shear flow ($\omega_E > 0$) oscillating states can be obtained (Fig. 5).

8. Conclusions

Oscillations of turbulent transport of particles and energy in magnetically confined plasmas can be easily observed in simulations of a variety of turbulence models. These oscillations typically involve a mechanism of energy exchange

between fluctuations and a poloidal shear flow. In the case of the RBM turbulence simulations presented here, a OD model can be constructed systematically that reproduces these oscillations.

However, the kind of "predator-prey" mechanism underlying these oscillations is found to be not relevant for transport barrier relaxations. In RBM turbulence simulations with transport barrier, relaxation oscillations of the latter are observed even in the case of frozen poloidal shear flow. These relaxations are due to a transitory growth of a mode localized at the center of the barrier. A 1D model for the evolution of such a mode in the presence of a shear flow describes a transitory growth of an initial perturbation. The corresponding time scale is large enough to allow for a significant growth in the case of low diffusivity and low poloidal wavenumber. This agrees well with the fact that the mode observed in the full simulations is located at the barrier center, where the diffusivity is close to the collisional value, and that its poloidal mode number is the lowest possible at that position.

The 1D evolution equation for the central mode does not explain, however, the repetition of relaxation events. After the initial growth, the amplitude decreases monotonically with time. In order to construct a model that allows for oscillating solutions, one has to take into account the coupling of the mode to the dynamics of the pressure profile. Such a coupled system of equations shows periodic oscillations in the case of a finite (steady state) shear flow. These oscillations are different from the quasi-periodic relaxation events observed in the full system. A possible way to reproduce these relaxation oscillations may be to include ambient noise in the 1D system. This work is still in progress.

References

[1] M. Bécoulet *et al.*, Plasma Phys. Control. Fusion **45**, A93 (2003).

[2] P. Beyer, S. Benkadda and X. Garbet, Phys. Rev. E **61**, 813 (2000).

[3] V. Naulin, J.J. Rasmussen and J. Nycander, Phys. Plasmas **10**, 1075 (2003).

[4] G. Manfredi and C.M. Roach, Phys. Plasmas **10**, 2824 (2003).

[5] P. Beyer, S. Benkadda, X. Garbet *et al.*, Phys. Rev. Lett. **85**, 4892 (2000).

[6] S. Benkadda, P. Beyer, N. Bian *et al.*, Nucl. Fusion **41**, 997 (2001).

[7] J.L. Lumley, *Atmospheric Turbulence and Radio Wave Propagation*, ed. A.M. Yaglom and V.I. Tatarski (Nauka, Moscow, 1967), p. 166.

[8] S. Benkadda, T. Dudok de Wit *et al.*, Phys. Rev. Lett. **73**, 3403 (1994).

[9] H. Biglari, P.H. Diamond and P.W. Terry, Phys. Fluids B **2**, 1 (1990).

[10] K.C. Shaing *et al.*, Phys. Fluids B **2**, 1492 (1990).

[11] A.S. Ware *et al.*, Plasma Phys. Control. Fusion **38**, 1343 (1996).

[12] C.F. Figarella, S. Benkadda, P. Beyer *et al.*, Phys. Rev. Lett. **90**, 015002 (2003).

[13] K.H. Burrell, Phys. Plasmas **6**, 4418 (1999).

[14] P.W. Terry, Rev. Mod. Phys. **72**, 109 (2000).

[15] R.J. Taylor *et al.*, Phys. Rev. Lett. **63**, 2365 (1989).

[16] R.R. Weynants *et al.*, Nucl. Fusion **32**, 837 (1992).

[17] J. Cornelis *et al.*, Nucl. Fusion **34**, 171 (1994).

[18] J.F. Drake *et al.*, Phys. Fluids B **4**, 488 (1992).

[19] J.M. Finn, J.F. Drake and P.N. Guzdar, Phys. Fluids B **4**, 2758 (1992).

[20] H. Sugama and W. Horton, Phys. Plasmas **1**, 345 (1994).